# Unimolecular Isomerization/Decomposition of Cyclopentadienyl and Related Bimolecular Reverse Process: *Ab Initio* MO/Statistical Theory Study

**L. V. MOSKALEVA, M. C. LIN**

*Department of Chemistry, Emory University, Atlanta, Georgia 30322*

*Received 20 January 1999; accepted 28 October 1999*

**ABSTRACT:** The cyclopentadienyl radical decomposition has been studied in detail by high-level correlation MO methods combined with multichannel RRKM rate constant calculations. The product channels of the reaction were examined by calculating their pressure-dependent branching rate constants. The overall reaction rate has been shown to be controlled by the first transition state corresponding to 1,2-hydrogen atom migration. Also, the reverse bimolecular reactions ($C_3H_3 + C_2H_2 \rightarrow$ products) have been included in the study. We provide a summary of pressure dependent rate constant expressions for the 1000–3000 K temperature range that may be useful for kinetic modeling of relevant combustion systems. © 2000 John Wiley & Sons, Inc. J Comput Chem 21: 415–425, 2000

**Keywords:** *ab initio*; MO; RRKM calculations

## Introduction

The relevance of the cyclopentadienyl (c-$C_5H_5$) radical to the formation of polycyclic aromatic hydrocarbons and soot in hydrocarbon combustion has gained increasing attention lately, thanks to the results of recent theoretical calculations. For example, the recombination of c-$C_5H_5$ and its cross-combination with $CH_3$[1, 2] have been shown by *ab initio* molecular orbital (MO) calculations to produce naphthalene and benzene, respectively, with ease. In hydrocarbon combustion, c-$C_5H_5$ can be directly produced from the decomposition of $C_6H_5O$ (phenoxy radical)[3–6] and from the reaction of $C_2H_2$ with $C_3H_3$ (propargyl radical), which are known to coexist near sooting conditions. The concentration of the $C_3H_3$ radical in the near sooting flame of $C_2H_2$,

*Correspondence to:* M. C. Lin; e-mail: chemmcl@emory.edu

Contract/grant sponsor: Department of Energy, Office of Basic Energy Sciences, Division of Chemical Sciences; contract/grant number: DE-FGO5-91ER14191

for example, has been estimated to be comparable to those of H and $CH_3$.[7] We have previously investigated the mechanism for the formation of $C_3H_4$ (propyne) from the $CH_3 + C_2H_2$ reaction, the most likely precursor process of $C_3H_3$,[8] which can be produced readily by the abstraction reactions, $X + C_3H_4 \rightarrow HX + C_3H_3$, where X = H, OH, $CH_3$, etc. The mechanism for the decomposition of the phenoxy radical producing $CO + c\text{-}C_5H_5$ has been studied theoretically in detail,[9, 10] whereas that for the decomposition of $c\text{-}C_5H_5$ or its reverse process, $C_3H_3 + C_2H_2$, is not well understood. This is the objective of the present investigation. Experimentally, the mechanism as well as the kinetics of the unimolecular decomposition of $c\text{-}C_5H_5$ have been studied very recently by two research groups with shock tubes.[11, 12] The kinetics for the formation of $C_2H_2 + C_3H_3$:

$$c\text{-}C_5H_5 \rightarrow C_2H_2 + C_3H_3 \qquad (1)$$

has been analyzed by assuming the involvement of different $C_5H_5$ intermediates. Our goal is to elucidate the mechanism for reaction (1) and to provide the combustion community a realistic estimate for its rate constant and those of potential isomerization reactions, which are believed to exist under varying T, P-conditions.

## Computational Methods

### MO CALCULATIONS

The geometry optimizations were performed at the density functional level using the B3LYP method (Becke's Three Parameter Hybrid Method[13] with the LYP Correlation Functional of Lee, Yang, and Parr[14]) with the 6-31G(d,p) basis set. Vibrational frequencies, calculated at this level, have been used for characterization of stationary points, zero-point energy (ZPE), and RRKM computations.

The reaction paths of the $C_5H_5 \leftrightarrow C_3H_3 + C_2H_2$ reaction were produced by complete optimization of structural parameters for the reactants, products, transition states, and intermediates. The energetics along the reaction paths were established by single-point energy computations with the higher level *ab initio* methods including the restricted open shell-coupled cluster, ROHF-CCSD(T),[15] the second-order multiconfigurational perturbation theory based on a CASSCF reference function, CASPT2,[16] and the G2M(rcc,MP2),[17] which is a modification of the Gaussian-2 (G2) scheme of Pople and coworkers.[18] Predicted energies for various species, including transition states, are summarized in Tables I–III. As can be seen from the results summarized in Table III, MPn methods did not work well for some intermediate structures and transition states involved in the $C_5H_5$ decomposition. This could be explained by the high spin contamination, which is a drawback of all unrestricted single-reference methods. Consequently, ROHF-CCSD(T) energies were adopted for further RRKM rate-constant calculations. The coupled-cluster family of methods proved to be very efficient in the accurate prediction of various molecular properties.[19] The CASPT2 technique is relatively new, but it appears to perform well with the same level of accuracy (see, e.g., Lindth et al.[20]), which is especially important for the systems that have an inherent multireference character.

The CASSCF calculations were performed with six orbital/seven electron active spaces and the 6-31G(d,p) basis set. In the subsequent CASPT2 calculations inner shells were not correlated.

In the part of the study dealing with the $c\text{-}C_5H_5$ heat of formation we applied and compared several high-level *ab initio* methods including G2M(RCC,MP2),[17] G2M(rcc,MP2), ROHF-CCSD(T), and CASPT2. Single-point energy calculations were based on the B3LYP/6-311G(d,p)-optimized geometries.

**TABLE I.**
**Calculated Total Energies (ZPE Corrected) in Hartrees of the $c\text{-}C_5H_5$ Radical and Reference Species.**

| | $c\text{-}C_5H_6$ | $C_6H_5$ | $C_6H_6$ | $c\text{-}C_5H_5$ |
|---|---|---|---|---|
| B3LYP/6-311G(d,p) | −194.15372 | −232.30855 | −231.61942 | −193.51298 |
| ROHF-CCSD(T)/6-31G(d,p) | −193.5374536 | −231.5719795 | −230.8884433 | −192.8980266 |
| ROHF-CCSD(T)/6-311G(d,p) | −193.6084063 | −231.6538394 | −230.9693673 | −192.96756 |
| CAS PT2/6-31G(d,p) | −193.4714922 | −231.3718654 | −230.6930404 | −192.83962 |
| G2(MP2) | −193.703697 | −231.776251 | −231.092001 | −193.069874 |
| G2M(rcc,MP2) | −193.7029536 | −231.7750267 | −231.1001119 | −193.0702904 |
| G2M(RCC,MP2) | −193.7054222 | −231.7781394 | −231.1033269 | −193.0730186 |

The GAUSSIAN 94,[21] MOLPRO 96[22] programs were employed for the MO computations.

## MULTICHANNEL RRKM CALCULATIONS

The multichannel RRKM calculations[23] for reaction (1) were performed based on the following detailed mechanism:

$$\begin{array}{ccccccc} \text{c-}C_5H_5^* & \overset{\text{-a}}{\underset{\text{a}}{\rightleftharpoons}} & C_5H_5(\mathbf{2})^* & \overset{\text{-b}}{\underset{\text{b}}{\rightleftharpoons}} & C_5H_5(\mathbf{3,4})^* & \xrightarrow{\text{c}} & C_3H_3 + C_2H_2 \\ \Big\downarrow\omega_1 & & \Big\downarrow\omega_2 & & \Big\downarrow\omega_3 & & \\ \text{c-}C_5H_5 & & C_5H_5(\mathbf{2}) & & C_5H_5(\mathbf{3,4}) & & \end{array}$$

$$C_5H_5(\mathbf{2})^* \overset{\text{-d}}{\underset{\text{d}}{\rightleftharpoons}} C_5H_5(\mathbf{6})^* \xrightarrow{\omega_4} C_5H_5(\mathbf{6})$$

where the asterisk represents internal excitation, and $\omega_j$ represents the effective quenching rate constant for the $j$th reaction step.

The geometries and identifications of various $C_5H_5$ isomers, transition states, and products are presented in Figure 1.

In the simplified scheme above, $C_5H_5(\mathbf{3,4})$ stands for all acyclic isomers except **6**, which is denoted as $C_5H_5(\mathbf{6})$. We treated the two pathways originating from **2** towards **3a** and **4** as degenerate, and ignored the geometric isomers of 1,3,4-pentatrieneyl (see Fig. 2). We also assumed the formation of **6** directly from **2** via **TS8**. The applicability of these assumptions is accounted for in the Results and Discussion section.

The thermally averaged unimolecular rate constants for all exit channels, with steady-state assumption, can be expressed as follows:

$$k_{\omega_2}(T) = Q\int_0^\infty \omega_2 YZ(E)ZZ(E)f(E^{\neq})\,dE^{\neq}$$

$$k_{\omega_3}(T) = Q\int_0^\infty \omega_3 XY(E)YZ(E)ZZ(E)f(E^{\neq})\,dE^{\neq}$$

$$k_{\omega_4}(T) = Q\int_0^\infty \omega_4 PY(E)YZ(E)ZZ(E)f(E^{\neq})\,dE^{\neq}$$

$$k_{A+B}(T) = Q\int_0^\infty k_c(E)XY(E)YZ(E)ZZ(E)f(E^{\neq})\,dE^{\neq}$$

where

$$Q = \frac{l_a^{\neq}}{h}\frac{Q_{tr}^{\neq}}{Q_{\text{c-}C_5H_5}}\exp\left(-E_a^0/RT\right)$$

$$XY(E) = k_b\Big/\left[k_{-b}(E) + k_c(E) + \omega_3\right]$$

$$PY(E) = k_d\Big/\left[k_{-d}(E) + \omega_4\right]$$

$$YZ(E) = 1\Big/\left[\omega_2 + k_b(E) + k_{-a}(E) + k_d(E) - k_{-b}(E)XY(E)\right]$$

$$ZZ(E) = \omega_1\Big/\left[\omega_1 + k_a(E) - k_{-a}(E)k_a(E)YZ(E)\right]$$

$$k_i(E) = l_i^{\neq}\frac{Q_i^{\neq}}{Q_j}\sum P_i\left(E_i^{\neq}\right)/hN_j(E),$$

$$i = a, -a, b, -b, c, d, -d;\ j = 1, 2, 3, 4$$

$$f(E^{\neq}) = \sum P_a\left(E_a^{\neq}\right)\exp\left(-E_a^{\neq}/RT\right)$$

where $k_{\omega_2}(T)$, $k_{\omega_3}(T)$, and $k_{\omega_4}(T)$ are the rate constants for deactivation of the excited adducts, whereas $k_{A+B}(T)$ is the thermal rate constant for the $C_3H_3 + C_2H_2$ formation from the two nearly degenerate A + B paths to be discussed later.

The observed overall rate constant for the c-$C_5H_5$ disappearance is given by the sum of individual rate constants:

$$k_t(T) = k_{A+B}(T) + k_{\omega_2}(T) + k_{\omega_3}(T) + k_{\omega_4}(T)$$

The effective quenching frequencies $\omega_j$ were estimated with Troe's weak-collision approximation[24] and expressed as $\omega_j = \beta_j Z_j[M]$, where $Z_j$ are the Lennard–Jones collision numbers and $\beta_j$ stand for the collision efficiencies. To estimate effective quenching frequencies, $\omega_j$, we used the effective Lennard–Jones parameters for $C_5H_5$ and Ar (which is assumed to be the diluent), $\sigma = 4.55$ Å and $\varepsilon/k = 197$ K, obtained by taking arithmetic and geometric mean of those for Ar ($\sigma = 3.465$ Å, $\varepsilon/k = 116$ K) and $C_6H_6$ ($\sigma = 5.628$ Å, $\varepsilon/k = 335$ K) taken from ref. 25.

In the equations above, "$\neq$" represents transition state quantities. $Q_{tr}^{\neq}$ is the product of the translational and rotational partition functions of the transition state associated with step ($a$). $E_a^0$ is the energy barrier with respect to the reactants for the step ($a$) at 0 K. $k_i(E)$ are the energy-specific decomposition or isomerization rate constant for the excited $C_5H_5(\mathbf{3,4})$, $C_5H_5(\mathbf{2})$, or c-$C_5H_5$ via step ($i$), with $i = -a, a, b, -b, c, d, -d$. $\sum P_i(E_i^{\neq})$ is the sum of states of the transition state $i$ with an excess energy $E_i^{\neq}$ above the transition state for process ($i$). $N_j(E)$ is the density of states of the intermediates with $j = 1$ for c-$C_5H_5$, $j = 2$ for $C_5H_5(\mathbf{2})$, $j = 3$ for $C_5H_5(\mathbf{3,4})$, and $j = 4$ for $C_5H_5(\mathbf{6})$. $Q_i^{\neq}$ and $Q_j$ are the overall rotational partition functions for transition states $i$ and intermediates $j$, with $i = -a, a, b, -b, c, d, -d$ and $j = 1, 2, 3, 4$.

The molecular properties of the reactants, products, intermediates, and transition states used in the RRKM calculations are given in Table IV. For the c-$C_5H_5$, we neglected the Jahn–Teller effect, and assumed $D_{5h}$ symmetry, which is justified by a low pseudorotation barrier and negligible degeneracy splitting, as indicated by several experimental and theoretical investigations.[26–29] It should be noted that for the elementary reactions ($a$) and ($-a$), the

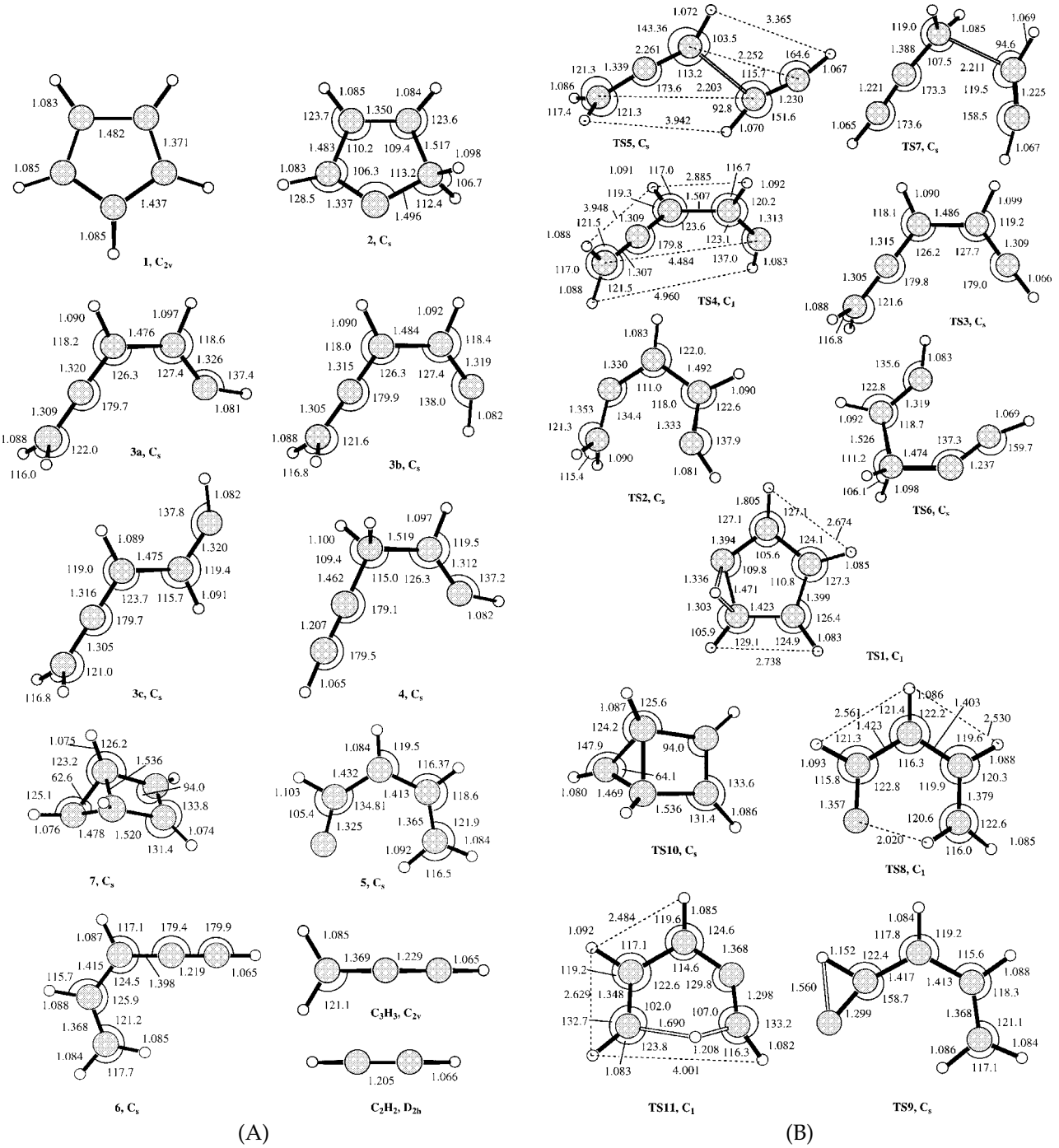


**FIGURE 1.** Optimized (B3LYP) molecular geometries (A) of the reactant, intermediates and products; (B) of the corresponding transition states.

statistical factors are not simply the ratios of the corresponding symmetry numbers. This is due to the fact that **TS1** does not have a symmetry plane, i.e., the migrating hydrogen atom can come from either side of the $C_5$ plane. As a result, $l^{\neq}_{-a} = 2$ and $l^{\neq}_{a} = 20$. For reaction (*a*), the ratio of electronic degeneracies introduces an additional factor of 1/2, because the ground state of c-$C_5H_5$, $E'_1$, is doubly degenerate. For reaction (*b*), the path degeneracy is 2, because we convoluted two pathways in one, and for the same reason it is 8 for the reaction (−*c*), which does not appear in the scheme above, but will be needed

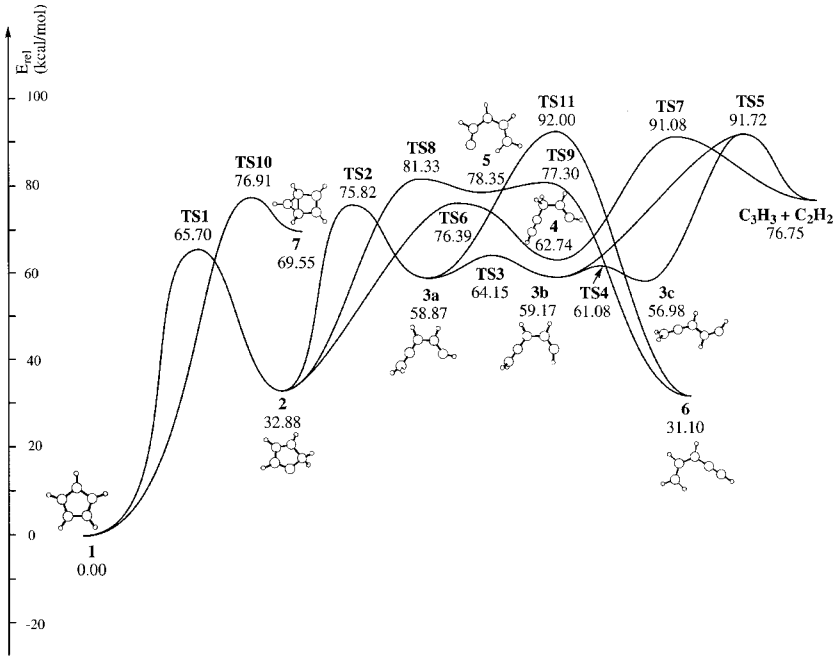


**FIGURE 2.** Potential energy diagram for the c-$C_5H_5$ radical isomerization/decomposition reaction. ZPE corrected energies are given as calculated at the RCCSD(T)/6-31G(d,p) level.

when the reverse process is considered (see Results and Discussion).

## Results and Discussion

### HEAT OF FORMATION OF THE $C_5H_5$ RADICAL

In the past few years, the question of the cyclopentadienyl heat of formation emerged several times due to the large uncertainty in the reported experimental measurements, which range roughly from 45 to 63 kcal/mol. The most recent experiments yielded $63 \pm 2$ kcal/mol from the ICR $C_5H_5^-$ basisity bracketing,[30] $61 \pm 2$ kcal/mol, from the ICR measurements of the $C_5H_6$ acidity[31] coupled with electron affinity determination,[32] and a lower value of $58 \pm 2$ kcal/mol derived from iodination study.[33] In 1991, Karni et al.[34] performed the first theoretical calculation at the HF/6-31G(d)//HF/3-21G level. Their result, 63.6 kcal/mol, is, surprisingly, in close agreement with more recent and more sophisticated calculation by Wang and Brezinsky,[29] who obtained $\Delta_f H^\circ_{298} = 62$ kcal/mol at the G2(B3LYP/MP2,SVP) level. Both groups used isodesmic reactions containing an ethyl radical, which may not be the best choice because of the existing uncertainty of about 1.5 kcal/mol in its heat of formation. In the present work we employed a different isodesmic reaction:

$$\text{c-}C_5H_6 + C_6H_5 \leftrightarrow \text{c-}C_5H_5 + C_6H_6 \qquad (2)$$

where the heats of formation of all the reference species are very well known (see Table II). For this reaction, we calculated the $\Delta H^\circ_0$ by various high level *ab initio* methods (Tables I and II). The thermal corrections in all cases were computed based on the B3LYP/6-311G(d,p) frequencies and moments of inertia. Following Wang and Brezinsky, we treated the lowest frequency vibrational mode of the $C_5H_5$ radical as a two-dimensional free rotor.

### ISOMERIZATION AND DECOMPOSITION OF THE $C_5H_5$ RADICAL

It is well established theoretically[27–29, 36] and experimentally[26, 37, 38] that the c-$C_5H_5$ radical undergoes Jahn–Teller distortion from $D_{5h}$ to $C_{2v}$ symmetry, and the resulting equilibrium structures, corresponding to $B_1$ and $A_2$ states, were reported to have nearly equal electronic energies.[27–29] As for the relative ordering of these two minima, no consensus has been reached, because it depended on the MO method employed. Experimentally, the reversed ordering was observed for two cyclopentadienyl isotopomers, $C_5H_4D$ and $C_5HD_4$.[38] However, the observed splitting of $\sim 9$ cm$^{-1}$, which should be mainly due to zero point energy splitting, can only

**TABLE II.**
**Enthalpy of Formation (kcal/mol) of the Cyclopentadienyl Radical Calculated at Various Levels of Theory.**

| | $\Delta_f H^\circ_0$ | $\Delta_f H^\circ_{298}$ |
|---|---|---|
| B3LYP/6-311G(d,p) | 65.22 | 62.56 |
| ROHF-CCSD(T)/6-31G(d,p) | 67.90 | 65.25 |
| ROHF-CCSD(T)/6-311G(d,p) | 68.21 | 65.55 |
| CAS PT2/6-31G(d,p) | 66.12 | 63.46 |
| G2(MP2) | 64.80 | 62.14 |
| G2M(rcc,MP2) | 69.93 | 67.27 |
| G2M(RCC,MP2) | 69.83 | 67.17 |
| Reference species | | |
| c-$C_5H_6$ | 36.23 | 32.1[a] |
| $C_6H_5$ | 84.3[c] | 81.26[b] |
| $C_6H_6$[b] | 23.83 | 19.86[a] |

Molecular Parameters[d] of c-$C_5H_5$ Used for the Thermal Correction Calculation

| Moments of Inertia, $10^{-40}$ g cm$^2$ | Symmetry Number | Vibrational Frequencies, cm$^{-1}$ |
|---|---|---|
| 91.116, 99.552, 190.669<br>I(free rotor) = 190.669 | 10 | 503, 517, 690, 722, 821, 843, 891, 899, 933, 954, 1067, 1083, 1150, 1227, 1307, 1404, 1509, 1554, 3217, 3223, 3235, 3252, 3260 |

[a] Ref. 35.
[b] Ref. 41.
[c] Ref. 42.
[d] Obtained at the B3LYP/6-311G(d,p) level of theory.

suggest that the splitting of classical electronic levels is also very small. This is what one expects for the case of linear Jahn–Teller coupling. Thus, we have arbitrarily chosen the $^2B_1$ as a reference, and computed all energies for this state, while in the statistical theory calculations we treated the ground electronic state of c-$C_5H_5$ as doubly degenerate.

The potential energy diagram for the $C_5H_5$ isomerization and dissociation is presented in Figure 2. The energies are given in kcal/mol at the ROHF-CCSD(T)/6-31G(d,p) and CASPT2/6-31G(d,p) levels.

The dissociation of the cyclopentadienyl radical to propargyl and acetylene is a multistep process. It involves as a first stage the 1,2-hydrogen atom shift producing 1,3-cyclopentadienyl radical, which is further referred to as **2** or $C_5H_5$(**2**). We found that the barrier for this process is 65.7, 61.9, and 62.4 kcal/mol at the ROHF-CCSD(T)/6-31G(d,p), CASPT2/6-31G(d,p), and G2M(rcc,MP2) levels, respectively. Intermediate **2** then undergoes a ring opening; at this point the reaction path splits. Depending on which bond of **2** is being broken, either (CCCC-*cis*, HCCH-*cis*) 1,3,4-pentatrienyl radical, **3a**, or 1-pentene-4-ynyl radical, **4**, can be formed. Both of them eventually lead to $C_3H_3 + C_2H_2$. In the following discussion labels (I) and (II) indicate the two respective pathways. **4** results from the acetylene addition to the $CH_2$ site of propargyl, whereas **3c** from the addition to the CH site; subsequent isomerization leads to **3a** via **3b**. The transition state **TS5** exhibits free rotation about the forming C—C bond; thus, we assume that both **3b** and **3c** can be directly formed. More detailed analysis shows that the three target diastereomers have nearly equal energies and the barriers for the internal rotation or *cis–trans* isomerization are of the order of 2 kcal/mol at the ROHF-CCSD(T)/6-31G(d,p) level, which allows us to treat them as one averaged minimum in the statistical theory calculations. One can notice that energywise the two pathways are nearly equivalent. This coincidence has been taken advantage of in our RRKM calculations.

We have also examined other possible routes of c-$C_5H_5$ decomposition not necessarily leading to $C_3H_3 + C_2H_2$. The intramolecular ring closure of the

cyclopentadienyl radical to give bicyclo[2.1.0]penta-2-en-5-yl requires a much higher energy than the 1,2-hydrogen shift. Consequently, any pathways originating from it can be ruled out.

In addition to the two discussed pathways commencing with the 1,3-cyclopentadienyl ring opening, there is another viable one through **TS8** (81.33 kcal/mol at the ROHF-CCSD(T) level) to a rather high lying 2,4-penten-1-yl-5-ylidene, **5**, which rearranges, to 2-penten-4-ynyl, **6**, stabilized by allylic resonance. Because **TS8** is still below **TS5** and **TS7**, the production of **6** may compete with the fragmentation to $C_3H_3 + C_2H_2$.

As can be noted from Table III, the relative energies, obtained at the four best levels including MP4, ROHF-CCSD(T), CASPT2, and G2M, are generally in close agreement, except perhaps, only intermediate **5**, for which PMP4 significantly overestimates the energy. Apparently, the PMP4 value is not very reliable because of high spin contamination of the UHF wave function. On the other hand, one can see that at the G2M level this deficiency is compensated, thanks to a favorable cancellation of errors, and the G2M relative energies are very close to ROHF-CCSD(T) energies, the latter method being free from spin contamination problems. It can also be seen from Table III that B3LYP/6-31G(d,p) works very well for this system: we notice that $\langle S^2 \rangle$ values are much better than those with the UHF wave function, and B3LYP relative energies are within 2 kcal/mol from those of G2M. This agreement is remarkable, because B3LYP energies are not included in the G2M computational scheme.

Following the procedure described in Computational Methods, we performed multichannel RRKM calculations for the overall c-$C_5H_5$ disappearance rate constant and branching rate constants for individual channels. The results are summarized in Table V. The overall rate constant for the c-$C_5H_5$ disappearance, $k_t$, at various pressures is plotted in Figure 3. We made one serious approximation: the two pathways, (I) and (II), were treated as degen-

**TABLE III.**
**Relative Energies (kcal/mol) of the Species and Transition States Involved in the Cyclopentadienyl Radical Decomposition.**

| Species and Transition States | ZPE[a] | B3LYP/ 6-31G(d,p) | PMP4/ 6-311G(d,p) | $\langle S^2 \rangle$ B3LYP | $\langle S^2 \rangle$ UHF | ROHF-CCSD(T)/ 6-31G(d,p) | CAS PT2/ 6-31G(d,p) [6:7] | G2M (rcc,MP2) |
|---|---|---|---|---|---|---|---|---|
| **1**($^2B_1$) | 49.02 | 0.00 | 0.00 | 0.77 | 1.00 | 0.00 | 0.00 | 0.00 |
| **TS1** | 47.77 | 61.94 | 61.84 | 0.80 | 0.95 | 65.70 | 61.90 | 62.39 |
| **2**($^2A'$) | 50.18 | 35.65 | 35.09 | 0.77 | 1.31 | 32.88 | 32.64 | 34.09 |
| **TS2** | 47.00 | 76.18 | 77.25 | 0.76 | 1.41 | 75.82 | 76.47 | 74.49 |
| **3a**($^2A'$) | 47.18 | 57.98 | 62.14 | 0.77 | 1.43 | 58.87 | 62.75 | 62.72 |
| **TS3** | 46.11 | 61.67 | 65.66 | 0.77 | 1.38 | 64.15 | 68.19 | 62.18 |
| **3b**($^2A'$) | 47.39 | 58.05 | 66.93 | 0.77 | 1.42 | 59.17 | 62.94 | 57.88 |
| **TS4** | 47.08 | 61.26 | 62.59 | 0.76 | 1.09 | 61.08 | 65.36 | 59.45 |
| **3c**($^2A'$) | 47.52 | 55.75 | 59.60 | 0.77 | 1.36 | 56.98 | 60.66 | 56.28 |
| **TS5** | 43.95 | 88.84 | 88.04 | 0.80 | 1.44 | 91.72 | 92.66 | 88.73 |
| **TS6** | 47.34 | 79.70 | 78.59 | 0.79 | 1.39 | 76.39 | 77.33 | 74.96 |
| **4**($^2A'$) | 47.28 | 66.56 | 63.69 | 0.77 | 0.97 | 62.74 | 66.34 | 60.85 |
| **TS7** | 43.99 | 90.74 | 91.03 | 0.79 | 1.32 | 91.08 | 90.89 | 86.97 |
| **$C_3H_3$**($^2B_1$) + **$C_2H_2$**($^1\Sigma_g$)[b] | 42.49 | 77.96 | 70.65 | 0.76 | 0.98 | 76.75 | 77.84 | 74.62 |
| **TS8** | 47.24 | 78.33 | 81.27 | 0.79 | 1.33 | 81.34 | 87.92 | 81.10 |
| **5** | 46.58 | 74.54 | 97.82 | 0.79 | 1.33 | 78.35 | 79.80 | 78.42 |
| **TS9** | 45.42 | 74.20 | 73.08 | 0.79 | 1.10 | 77.30 | 78.78 | 75.33 |
| **6** | 47.77 | 28.90 | 27.92 | 0.79 | 1.17 | 31.10 | 31.82 | 29.64 |
| **TS10** | 51.11 | 79.86 | 76.33 | 0.75 | 0.77 | 76.91 | 76.54 | 75.97 |
| **7** | 49.07 | 72.71 | 69.29 | 0.75 | 0.76 | 69.55 | 68.83 | 68.57 |
| **TS11** | 44.65 | 89.90 | 95.70 | 0.85 | 2.04 | 92.00 | 90.95 | 96.30 |

[a] ZPE is calculated at the B3LYP/6-31G(d,p) level.
[b] The total energies (in hartree) for the $C_5H_5$ are: B3LYP/6-31G(d,p), −193.47057; PMP4/6-31G(d,p), −192.89926; PMP4/6-311G(d,p), −192.970001; MP2/6-311G(d,p), −192.88345; MP2/6-311+G(3df,2p), −193.00097; ROHF-CCSD(T)/6-31G(d,p), −192.89811; CASPT2/6-31G(d,p)[6:7], −192.83962.

**TABLE IV.**
**Molecular and Transition-State Parameters Used for RRKM.**

| Species or Transition State | $E_{rel}$,[a] kcal/mol | Symmetry Number | Moments of Inertia, $10^{-40}$ g cm$^2$ | Vibrational Frequencies, cm$^{-1}$ |
|---|---|---|---|---|
| **c-$C_5H_5$** | 0.00 | 10 | 91.12; 99.55; 190.67 | 26, 503, 517, 690, 722, 821, 843, 891, 899, 933, 954, 1067, 1083, 1150, 1227, 1307, 1404, 1509, 1554, 3217, 3223, 3235, 3252, 3260 |
| **TS1** | 65.70 | 1 | 80.47; 200.64; 281.11 | 591i, 137, 226, 353, 504, 566, 620, 683, 807, 847, 861, 942, 1025, 1127, 1263, 1334, 1396, 1485, 1592, 3018, 3060, 3169, 3195, 3265 |
| **$C_5H_5$(2)** | 32.88 | 1 | 91.76; 102.52; 189.04 | 309, 457, 676, 783, 797, 827, 911, 936, 944, 959, 1001, 1112, 1123, 1225, 1257, 1349, 1429, 1560, 1651, 3044, 3075, 3203, 3232, 3238 |
| **TS8** | 81.33 | 1 | 89.86; 141.92; 226.28 | 310i, 306, 441, 489, 562, 694, 710, 813, 860, 915, 979, 1042, 1094, 1127, 1245, 1388, 1424, 1523, 1565, 3122, 3134, 3171, 3204, 3237 |
| **$C_5H_5$(6)** | 31.10 | 1 | 61.86; 249.08; 310.94 | 161, 233, 387, 461, 505, 564, 629, 655, 740, 854, 951, 998, 1041, 1165, 1268, 1426, 1441, 1560, 2117, 3162, 3169, 3180, 3265, 3485 |
| **TS2** | 75.82 | 1 | 94.31; 138.55; 227.13 | 454i, 256, 404, 525, 527, 663, 681, 835, 849, 859, 891, 982, 1001, 1114, 1218, 1324, 1477, 1619, 1814, 3118, 3124, 3192, 3217, 3266 |
| **$C_5H_5$(3,4)** (average) | 58.34 | 1 | 41.06; 310.49; 345.78 | 123, 169, 349, 386, 526, 601, 679, 831, 874, 886, 913, 975, 1036, 1152, 1267, 1370, 1485, 1639, 2039, 3089, 3129, 3149, 3199, 3261 |
| **TS5** | 91.72 | 1 | 40.95; 390.31; 425.45 I(free rot.)=16.6 | 549i, 33, 120, 255, 298, 383, 486, 550, 614, 699, 758, 771, 780, 866, 1036, 1158, 1481, 1866, 1970, 3147, 3231, 3376, 3389, 3475 |
| **$C_3H_3$** | 15.91 | 2 | 2.91; 88.90; 91.81 | 367, 386, 436, 596, 677, 1037, 1100, 1474, 2027, 3159, 3249, 3482 |
| **$C_2H_2$** | 27.50 | 2 | 0.0; 23.97; 23.97 | 563, 563, 773, 773, 2086, 3437, 3536 |

[a] Energies relative to the reactants are given as calculated by ROHF-CCSD(T)/6-31G(d,p)//B3LYP/6-31G(d,p); the geometries and vibrational frequencies are computed at the B3LYP/6-31G(d,p) level of theory.

erate. However, the use of such an approximation was justified by comparing the rate constants calculated for each of them individually: the difference was small. We could see that, contrary to our expectations, the reaction rate is controlled by the first transition state **TS1**, rather than **TS5** and **TS7**. This suggests that we could safely convolute two separate pathways (I) and (II) into one. The results are consistent with the upper limit for $k_t$ at 623 K estimated by Alkemade and Homann[39] ($k < 1.00 \times 10^{11}$). The formation of **6** was assumed directly from **2** through **TS8**, because the isomerization barrier

**TABLE V.**

**Branching Rate Coefficients[a] for Individual Channels in Forward and Reverse Directions at the 1000–3000 K Temperature Range.**

| Reaction | 100 Torr | 1 atm | 10 atm |
|---|---|---|---|
| $C_3H_3 + C_2H_2 \rightarrow C_5H_5$(**3,4**) | $6.87 \times 10^{71}T^{-18.2}e^{-22827/T}$ | $4.11 \times 10^{72}T^{-18.2}e^{-22866/T}$ | $1.15 \times 10^{77}T^{-19.1}e^{-24974/T}$ |
| $C_5H_5$(**3,4**) $\rightarrow C_3H_3 + C_2H_2$ | $3.12 \times 10^{82}T^{-20.6}e^{-34674/T}$ | $1.95 \times 10^{83}T^{-20.6}e^{-34719/T}$ | $5.61 \times 10^{87}T^{-21.5}e^{-36832/T}$ |
| $C_3H_3 + C_2H_2 \rightarrow C_5H_5$(**2**) | $1.34 \times 10^{68}T^{-16.9}e^{-25953/T}$ | $2.70 \times 10^{53}T^{-12.6}e^{-20869/T}$ | $1.81 \times 10^{35}T^{-7.6}e^{-38474/T}$ |
| $C_3H_5$(**2**) $\rightarrow C_3H_3 + C_2H_2$ | $3.40 \times 10^{80}T^{-19.2}e^{-51467/T}$ | $7.48 \times 10^{65}T^{-15.0}e^{-46402/T}$ | $4.57 \times 10^{47}T^{-9.9}e^{-25953/T}$ |
| $C_3H_3 + C_2H_2 \rightarrow$ c-$C_5H_5$ | $6.17 \times 10^{66}T^{-15.7}e^{-24033/T}$ | $6.87 \times 10^{55}T^{-12.5}e^{-21148/T}$ | $1.13 \times 10^{43}T^{-8.8}e^{-17615T}$ |
| c-$C_5H_5 \rightarrow C_3H_3 + C_2H_2$ | $2.79 \times 10^{79}T^{-18.3}e^{-65845/T}$ | $1.98 \times 10^{68}T^{-15.0}e^{-62852/T}$ | $5.70 \times 10^{54}T^{-11.1}e^{-58849/T}$ |
| c-$C_5H_5 \rightarrow C_5H_5$(**2**) | $5.17 \times 10^{80}T^{-20.4}e^{-48407/T}$ | $5.92 \times 10^{78}T^{-19.5}e^{-48661/T}$ | $1.32 \times 10^{78}T^{-19.0}e^{-49916/T}$ |
| c-$C_5H_5 \rightarrow C_5H_5$(**3,4**) | $2.25 \times 10^{108}T^{-28.2}e^{-64328/T}$ | $1.21 \times 10^{109}T^{-28.1}e^{-65637/T}$ | $2.08 \times 10^{112}T^{-28.6}e^{-68944/T}$ |
| c-$C_5H_5 \rightarrow C_5H_5$(**6**) | $1.64 \times 10^{96}T^{-23.5}e^{-69154/T}$ | $2.52 \times 10^{80}T^{-18.9}e^{-65008/T}$ | $4.33 \times 10^{56}T^{-12.1}e^{-57338/T}$ |

[a] The units are $cm^3\ mol^{-1}\ s^{-1}$ for bimolecular reactions and $s^{-1}$ for unimolecular reactions. The calculations were performed based on the ROHF-CCSD(T) energies with B3LYP molecular parameters.

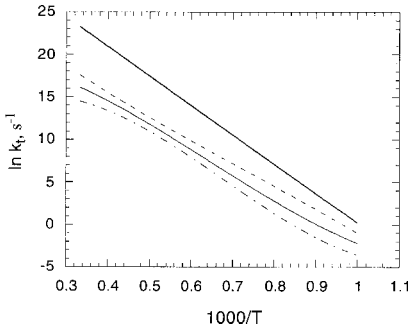


**FIGURE 3.** Calculated unimolecular rate constants for the c-$C_5H_5$ loss at different pressures. Solid bold curve: high pressure limit; dashed curve: 10 atm; solid plain curve: 1 atm; dash-dotted curve: 100 Torr.

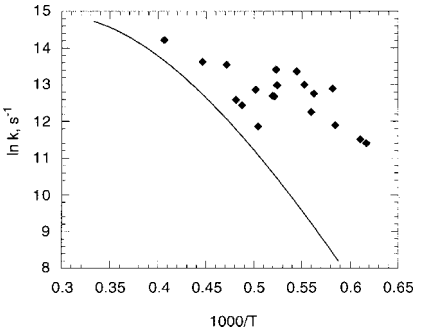


**FIGURE 4.** Comparison of the calculated RRKM rate constant for the c-$C_5H_5 \rightarrow C_2H_2 + C_3H_3$ reaction with the experimental data of Kiefer et al. (100–200 Torr). The RRKM calculation was carried out for 150 Torr.

from **5** to **6**, **TS9** was found to be negligible. Finally, we can point to the pronounced pressure effect on the total disappearance rate coefficient as well as those for branching fractions especially at high temperatures.

The comparison with the experimental results of Kiefer et al.[11] for overall reaction (1) is given in Figure 4 for the 150 Torr pressure and 1700–3000 K temperature range. Taking into account large experimental scatter, the agreement is satisfactory. In their modeling, Kiefer et al. assumed that reaction (1) proceeds in a single step, which is a rather severe approximation. Indeed, the experimental $C_2H_2$ concentration profile exhibits an initial induction period of about 0.1 ms that indicates a multistep process.

Frank et al.[12] assumed the decyclization transition state (**TS2**, **TS6**, **TS8** in the present work) to be rate determining, contrary to our conclusions. For kinetic modeling they used high-pressure limit rate constants, which must be a poor approximation also, because the RRKM calculations reveal significant pressure dependence for the overall process as well as for elementary steps.

Burcat and Dvinyaninov[40] in their modeling of the cyclopentadiene decomposition, derived the rate constant for the reaction c-$C_5H_5 \rightarrow C_5H_5$(**6**) (based on the concentration profiles of the decomposition products). Comparison with our results indicates a significant deviation, as shown in Figure 5.

## FORMATION OF THE $C_5H_5$ ISOMERS FROM $C_3H_3 + C_2H_2$

In addition, we performed RRKM calculations for the $C_3H_3 + C_2H_2$ reaction leading to the formation of c-$C_5H_5$ along with other $C_5H_5$ isomers using

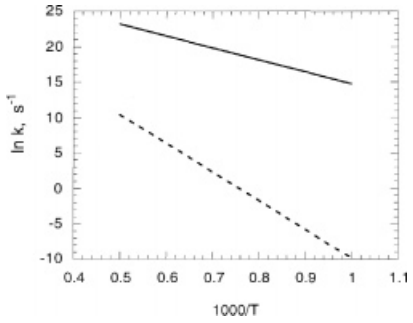


**FIGURE 5.** Arrhenius plot of the rate constant describing the production of $C_5H_5$(**6**) from c-$C_5H_5$. Solid line is the rate constant derived from modeling by Burcat et al., dashed line is the RRKM result for 5 atm.

the following mechanistic scheme:

$$C_3H_3 + C_2H_2 \underset{c}{\overset{-c}{\rightleftharpoons}} C_5H_5(\mathbf{3,4})^* \underset{b}{\overset{-b}{\rightleftharpoons}} C_5H_5(\mathbf{2})^* \underset{a}{\overset{-a}{\rightleftharpoons}} \text{c-}C_5H_5^*$$
$$\downarrow\omega_3 \qquad\qquad \downarrow\omega_2 \qquad\qquad \downarrow\omega_1$$
$$C_5H_5(\mathbf{3,4}) \qquad\qquad C_5H_5(\mathbf{2}) \qquad\qquad \text{c-}C_5H_5$$

The RRKM formulation for the chemically activated multichannel process has been derived in close analogy to that described in Computational Methods. Figure 6 presents the rate constant $k_t'$ as a function of temperature and pressure; the expressions for product branching rate constants are summarized in Table V.

Based on the microscopic reversibility principle, we also calculated pressure dependent rate constants for the reverse reactions, $C_5H_5(\mathbf{2}) \rightarrow C_3H_3 + C_2H_2$, and $C_5H_5(3,4) \rightarrow C_3H_3 + C_2H_2$ (see Table V), from the $\Delta G°(T)$ and respective reverse reaction rate constants.

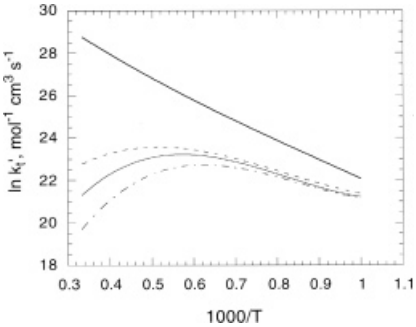


**FIGURE 6.** Calculated bimolecular rate constants for the $C_3H_3$ loss at different pressures. Solid bold curve: high pressure limit; dashed curve: 10 atm; solid plain curve: 1 atm; dash-dotted curve: 100 Torr.

## Concluding Remarks

The cyclopentadienyl radical isomerization/decomposition was investigated by means of the *ab initio* MO theory. The potential energy profiles were obtained with the high-level correlation *ab initio* methods, ROHF-CCSD(T), CASPT2, and G2M. A close agreement between the multireference CASPT2 and single-reference ROHF-CCSD(T) and G2M supports the reliability of our results.

Based on the calculated energetics and molecular parameters, RRKM calculations of the pressure-dependent rate coefficients were performed in both forward and reverse directions for overall rates and individual channels. We provided a summary of the rate coefficients for the 1000–3000 K temperature range at 100 Torr, 1 atm, 10 atm, which may be useful for kinetic modeling of the cyclopentadienyl and its parent cyclopentadiene decomposition processes.

Also, as a part of this study, we calculated the c-$C_5H_5$ heat of formation using an isodesmic reaction at several high levels of theory. All the results support the higher experimental value for the cyclopentadienyl radical heat of formation, $\Delta_f H°_{298} = 63 \pm 2$ kcal/mol.

## Acknowledgment

We are thankful to the Cherry L. Emerson Center for Scientific Computation for the use of various programs and computing facilities.

## References

1. Melius, C.; Colvin, M. E.; Marinov, N. M.; Pitz, W. J.; Senkan, S. M. 26th Symposium of the International Combusttion Proceedings, 1996, p. 685.
2. Moskaleva, L. V.; Mebel, A. M.; Lin, M. C. 26th Symposium of the International Combustion Proceedings, 1996, p. 521.
3. Glassman, I. Combustion; Academic Press: New York, 1985, 2nd ed.
4. Colussi, A. J.; Zabel, F.; Benson, S. W. Int J Chem Kinet 1977, 9, 161.
5. Lin, C.-Y.; Lin, M. C. J Phys Chem 1986, 90, 425.
6. Frank, P.; Herzler, J.; Just, Th.; Wahl, C. 25th Sympsoium of the International Combusttion Proceedings, 1994, p. 833.
7. Westmoreland, P. R.; Dean, A. M.; Howard, J. B.; Longwell, J. P. J Phys Chem 1989, 93, 8171.
8. Diau, E. W.; Lin, M. C.; Melius, C. F. J Chem Phys 1994, 101, 3923.

9. Olivella, S.; Sole, A.; Garcia-Raso, A. J Phys Chem 1995, 99, 10549.
10. Liu, R.; Morokuma, K.; Mebel, A. M.; Lin, M. C. J Phys Chem 1996, 100, 9314.
11. Kern, R. D.; Yao Zhang, J.; Jursic, B. S.; Tranter, R. S.; Greybill, M. A.; Kiefer, J. H. 27th Symposium of the International Combustion Proceedings, 1998.
12. Roy, K.; Horn, C.; Frank, P.; Slutsky, V. G.; Just, T. 27th Symposium of the International Combusttion Proceedings, 1998.
13. Becke, A. D. J Chem Phys 1993, 98, 5648.
14. Lee, C.; Yang, W.; Parr, R. G. Phys Rev B 1988, 37, 785.
15. Watts, J. D.; Gauss, J.; Bartlett, R. J. J Chem Phys 1993, 98, 8718.
16. Andersson, K.; Malmqvist, P. A.; Roos, B. O.; Sadlej, A. J.; Wolinski, K. J Phys Chem 1990, 94, 5483.
17. Mebel, A. M.; Morokuma, K.; Lin, M. C. J Chem Phys 1995, 103, 7414.
18. (a) Curtiss, L. A.; Raghavachari, K.; Trucks, G. W.; Pople, J. A. J Chem Phys 1991, 94, 7221; (b) Pople, J. A.; Head-Gordon, M.; Fox, D. J.; Raghavachari, K.; Curtiss, A. J Chem Phys 1989, 90, 5622; (c) Curtiss, L. A.; Jones, C.; Trucks, G. W.; Raghavachari, K.; Pople, J. A. J Chem Phys 1990, 93, 2537.
19. Lee, T. J.; Scuseria, G. E. Understand Chem React 1995, 13, 47.
20. Lindth, R.; Lee, T. J.; Bernhardson, A.; Persson, B. J.; Karlstorm, G. J Am Chem Soc 1987, 117, 7186.
21. Frisch, M. J.; Trucks, G. W.; Schlegel, H. B.; Gill, P. M. W.; Johnson, B. G.; Robb, M. A.; Cheeseman, J. R.; Keith, T.; Petersson, G. A.; Montgomery, J. A.; Raghavachari, K.; Al-Laham, M. A.; Zakrzewski, V. G.; Ortiz, J. V.; Foresman, J. B.; Cioslowski, J.; Stefanov, B. B.; Nanayakkara, A.; Challacombe, M.; Peng, C. Y.; Ayala, P. Y.; Chen, W.; Wong, M. W.; Andres, J. L.; Replogle, E. S.; Gomperts, R.; Martin, R. L.; Fox, D. J.; Binkley, J. S.; Defrees, D. J.; Baker, J.; Stewart, J. P.; Head-Gordon, M.; Gonzalez, C.; Pople, J. A. GAUSSIAN 94, revision A.1; Gaussian, Inc., Pittsburgh, PA, 1995.
22. MOLPRO is a package of *ab initio* programs written by H.-J. Werner and P. J. Knowles, with contributions from J. Almlöf, R. D. Amos, A. Berning, D. L. Cooper, M. J. O. Deegan, A. J. Dobbyn, F. Eckert, S. T. Elbert, C. Hampel, R. Lindh, A. W. Lloyd, W. Meyer, A. Nicklass, K. Peterson, R. Pitzer, A. J. Stone, P. R. Taylor, M. E. Mura, P. Pulay, M. Schütz, H. Stoll, and T. Thorsteinsson.
23. Diau, E. W.; Yu, T.; Wagner, A. G.; Lin, M. C. J Phys Chem 1994, 98, 4034.
24. Troe, J. J Chem Phys 1977, 66, 4745.
25. Stiel, L. I.; Thodos, G. J Chem Eng Data 1962, 7, 234.
26. (a) Liebling, G. H.; McConnell, H. M. J Chem Phys 1965, 42, 3931; (b) Hedaya, E. Acc Chem Res 1969, 2, 367.
27. Borden, W. T.; Davidson, E. R. J Am Chem Soc 1979, 101, 3771.
28. Pierloot, K.; Persson, B. J.; Joakim, B. O. J Phys Chem 1995, 99, 3465.
29. Wang, H.; Brezinsky, K. J Phys Chem A 1998, 102, 3334.
30. DeFrees, D. J.; McIver, R. T.; Hehre, W, J. J Am Chem Soc 1980, 102, 3334.
31. (a) Bartmess, J. E.; Scott, J. A.; McIver, R. T. J Am Chem Soc 1979, 101, 6046; (b) Cumming, J. B.; Kebarle, P. Can J Chem Phys 1978, 56, 1.
32. Engelking, P. C.; Linberger, W. C. J Chem Phys 1977, 67, 1412.
33. (a) McMillen, D. F.; Golden, D. M. Annu Rev Phys Chem 1982, 33, 493; (b) Puttemans, J. P.; Smith, G. P.; Golden, D. M. J Phys Chem 1990, 94, 3227.
34. Karni, M.; Oref, I.; Burcat, A. J Phys Chem Ref Data 1991, 20, 665.
35. Stull, D. R. The Chemical Thermodynamics of Organic Compounds; J. Wiley: New York, 1969.
36. (a) Meyer, R.; Graf, F.; Ha, T.-K.; Günthard, Hs. H. Chem Phys Lett 1979, 66, 65; (b) Ha, T.-K.; Meyer, R.; Günthard, Hs. H. Chem Phys Lett 1980, 69, 510.
37. Yu, L.; Foster, S. C.; Williamson, J. M.; Heaven, M. C.; Miller, T. A. J Phys Chem 1988, 92, 4263.
38. Yu, L.; Cullin, D. W.; Williamson, J. M.; Miller, T. A. J Chem Phys 1993, 98, 2682.
39. Alkemade, U.; Homann, K. H. Z Phys Chem 1989, 161, 19.
40. Burcat, A.; Dvinyaninov, M. Int J Chem Kinet 1997, 29, 505.
41. Nicolaides, A.; Smith, D.; Jensen, F.; Radom, L. J Am Chem Soc 1997, 119, 8083.
42. Davico, G. E.; Bierbaum, V. M.; DePuy, C. H.; Ellison, G. B.; Squires, R. R. J Am Chem Soc 1995, 117, 2590.